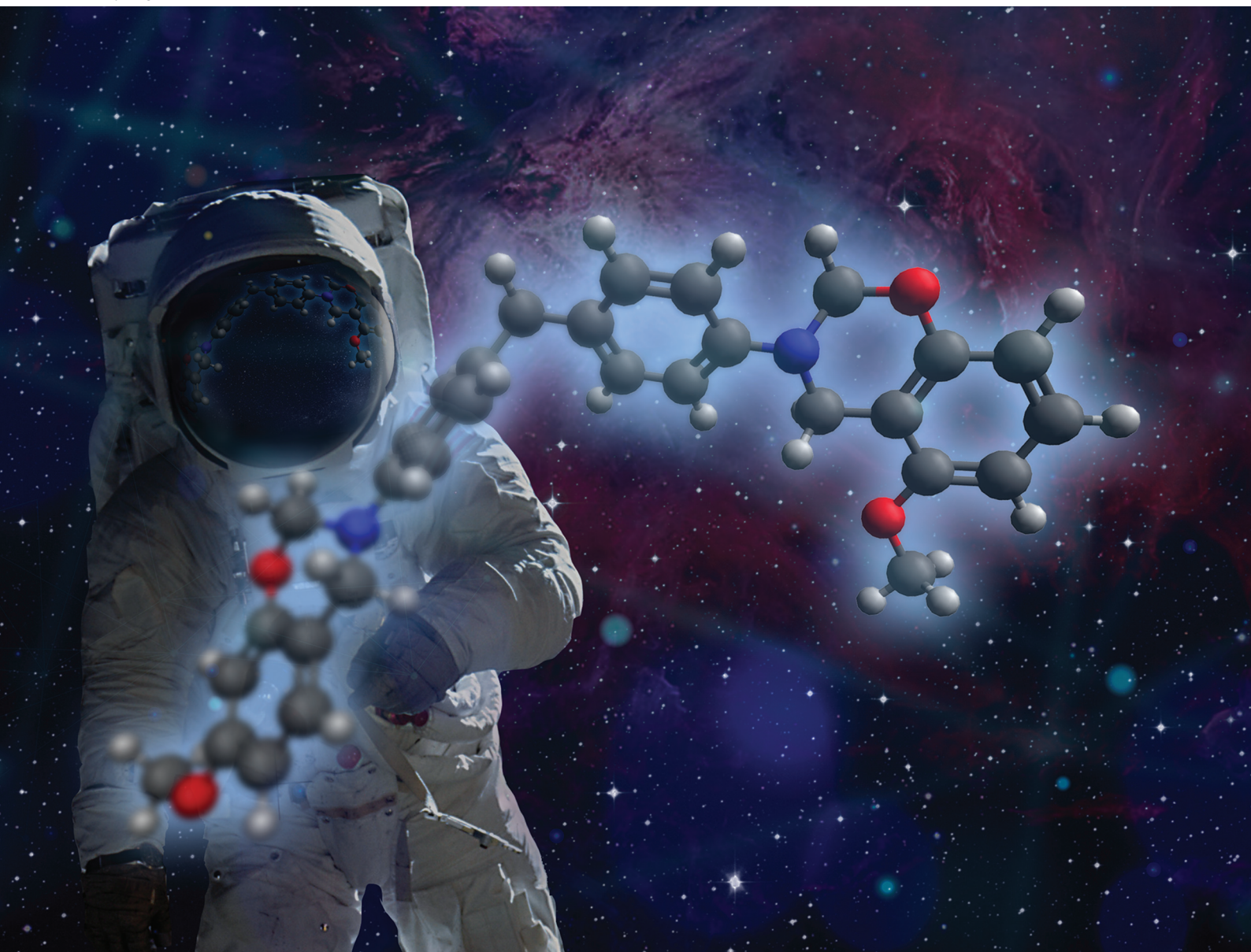


Polymer Chemistry

rsc.li/polymers

Volume 11
Number 4
28 January 2020
Pages 755-946



ISSN 1759-9962

PAPER

Hatsuo Ishida *et al.*
Electronic effects of asymmetric and meta-alkoxy
substituents on the polymerization behavior of
bis-benzoxazines



Cite this: *Polym. Chem.*, 2020, **11**, 800

Electronic effects of asymmetric and meta-alkoxy substituents on the polymerization behavior of bis-benzoxazines

Ya Lyu,^{a,b} Eric Rachita,^a Nicholas Pogharian,^a Pablo Froimowicz^c and Hatsuo Ishida^{*a}

Three isomers of benzoxazine monomers based on *m*-alkoxyphenol and 4,4'-methylenedianiline were synthesized and successfully isolated by column chromatography. The molecular structures of benzoxazine monomers were confirmed by proton nuclear magnetic resonance (¹H NMR) and Fourier-transform infrared (FT-IR) spectroscopy. The polymerization behavior evaluated by differential scanning calorimetry (DSC) shows that the asymmetric isomer, which has a methoxy group at the 5-position and 7-positions (5,7'MO-ddm), has only one exothermic peak between temperatures of the other two symmetric isomers. The ¹H NMR spectrum of monomers shows that the type and position of alkoxy groups can exert different effects on the electron density of the oxazine ring, and may result in a sensitive trend of ring-opening. The difference in electron densities was verified by the Gaussian simulation calculation results of natural charges. In this work, we provide a fundamental molecular-level understanding of the polymerization mechanism of asymmetric bis-benzoxazines, which can provide possibilities for designing new benzoxazines in order to solve the potential disadvantages of benzoxazines/polybenzoxazines and/or enhance their advantages.

Received 31st October 2019,
Accepted 22nd November 2019

DOI: 10.1039/c9py01641d

rsc.li/polymers

1 Introduction

Material researchers and industries have been greatly interested in benzoxazine resins and their crosslinked counterpart, polybenzoxazines, because of their well-balanced physical and mechanical properties. Furthermore, because of their excellent thermal stability and mechanical strength along with vast molecular design flexibility, they can overcome several shortcomings of conventional resins while retaining their advantages.^{1–5} The striking properties of polybenzoxazines include fire resistance,^{6–11} high char yield,¹² low water absorption,¹³ high mechanical strength,¹³ high glass transition temperatures (*T*_g),¹⁴ no or limited shrinkage upon polymerization^{13,15–17} and no major reaction byproduct formation during polymerization.⁴ However, polybenzoxazines, formed from mono-oxazine benzoxazine monomers, still have the disadvantages of typical monomer-based thermosetting

resins, such as brittleness, although this problem has been lessened using the so-called main-chain type, side-chain type, or telechelic polybenzoxazine precursors.^{18–20}

Polymers from mono-oxazine benzoxazines normally have a low molecular weight of approximately 4000 g mol^{−1} or less because of low crosslinking, which comes from the competition between the thermal dissociation or intramolecular hydrogen bond formation and the chain propagation of monomer.^{21,22} As a result, mono-oxazine benzoxazines are rarely used as high-performance materials. Difunctional benzoxazines allow crosslinking to yield polymers with an infinite molecular weight and, therefore, can be processed to shaped materials with excellent mechanical strengths.^{23–25} Bis-benzoxazines provide design versatility and flexibility not only because of a large number of diphenols and diamines with different bridging groups that are readily available, but also because the attachment of different functional groups at different positions on benzene rings is possible.²⁶ These are the two main factors affecting the ring-closing reaction of benzoxazine, and consequently affect its ability to participate in ring-opening polymerization.^{27–29} Promising solutions to enhance the properties of polybenzoxazines and tailor their processing conditions come from the nature of the substitution of the bridged and lateral groups forming the particular functionality of the benzoxazines.

^aDepartment of Macromolecular Science and Engineering, Case Western Reserve University, Cleveland, Ohio 44106-7202, USA. E-mail: hxi3@cwru.edu

^bResearch Center of Petroleum Processing, East China University of Science and Technology, Shanghai 200237, China

^cDesign and Chemistry of Macromolecules Group, Institute of Technology in Polymers and Nanotechnology (ITPN), UBA-CONICET, FIUBA, FADU, University of Buenos Aires, Pabellón III, subsuelo, Ciudad Universitaria, 1428 Buenos Aires, Argentina

Electronic effects, consisting of the withdrawing or donating of bridging groups and lateral groups, are important factors that act on thermal activation, the yield of the synthesis, and the properties of polybenzoxazines. Wang *et al.*³⁰ discussed in detail six bis-benzoxazines based on bisphenols with different bridging groups, $-\text{C}(\text{CH}_3)_2-$, $-\text{CH}_2-$, $-\text{O}-$, $-\text{CO}-$, $-\text{SO}_2-$, and single bonds. The electron-withdrawing groups promoted thermally activated polymerization and decreased polymerization temperatures by increasing the bond length and lowering the bond energy of C–O on oxazine rings. Ohashi *et al.*³¹ evaluated the effect of the substituents on their polymerization behavior through the systematic variation of the electronic properties of substituents in order to evaluate their effects on the polymerization process of benzoxazines. The electron-withdrawing groups introduced at the *para*-position of phenolic OH were nitro (NO_2), cyano (CN), trifluoromethyl, aldehyde (CHO), trifluoromethoxy (OCF_3), chloro (Cl), bromo (Br), and fluoro (F) groups, and the electron-donating groups were methylthio (SMe), phenyl (C_6H_5), methyl (CH_3), isopropyl (iPr), *tert*-butyl (*t*Bu), ethoxy (OCH_2CH_3), methoxy (OCH_3), and butoxy ($\text{OCH}_2\text{CH}_2\text{CH}_2\text{CH}_3$). Increased electron withdrawal of the *para*-substituent on phenol lowers the polymerization temperature.

Previous work demonstrated that the positions of substituted functional groups affect the ring-opening behavior and properties of polybenzoxazine. The *ortho*- and *para*-position amide benzoxazines induce intramolecular hydrogen bonding between the amide proton and the oxygen atom of the oxazine ring, which results in significant differences in their polymerization temperatures.³² The presence of a methylol group accelerates the ring-opening polymerization and decreases polymerization temperatures followed by the order of the *para*-, *meta*-, and *ortho*-positions.^{33,34} *m*-Alkoxyphenol was chosen for synthesis with linear aliphatic diamine, and the formed benzoxazine monomers presented ultra-low polymerization temperature, low viscosity, and good shelf life.³⁵

Designing asymmetric bis-benzoxazine monomers by adding different functionalities to benzoxazine monomers could be a new approach to achieve desirable properties of polybenzoxazines. An asymmetric bis-benzoxazine monomer was synthesized by aminophenol in which both OH and the primary amino formed an oxazine ring. Asymmetric benzoxazine, *n*-hexyl-benzoxazine, and *n*-butyl-benzoxazine have exhibited T_p in the range of 210–240 °C.³⁶ Dumas *et al.*³⁷ synthesized asymmetric benzoxazine monomers from phenol, eugenol, and 1,4-phenylenediamine. Puchot *et al.*³⁸ designed an asymmetric bio-based bis-benzoxazine monomer based on vanillin and cardanol, which exhibited a lower melting point similar to that of cardanol-based benzoxazine and a T_p similar to that of a vanillin- and cardanol-based benzoxazine. A similar synthesis approach was also performed with guaiacol and cardanol to obtain an asymmetric monomer.²⁵ Very interestingly, a single exothermic peak in the differential scanning calorimetry (DSC) curve thermogram is commonly observed despite the possibility of the existence of different oxazine structures, which indicates that all the ring-opening polymerization

occurs at the same time rather than separately. Ganfoud *et al.*³⁹ synthesized asymmetric card-phenol, which exhibits multi-exothermic peaks, but they explained that this phenomenon indicates the degradation of the long carbon chain.

To summarize, certain *meta*-position functional groups accelerate the effects on the ring-opening character of benzoxazine monomers and the properties of polybenzoxazines, while they can also create asymmetric benzoxazines with bi-amine diamines. Motivated by these facts, this work aims to study the benzoxazine monomers synthesized with di-aniline and *m*-methoxyphenol or *m*-butoxyphenol, in order to explore the electronic effect of meta-groups and the polymerization mechanism of asymmetric benzoxazines. Due to the asymmetric nature of the phenol, the synthesized monomer contains a mixture of isomers. The pure isomers, which are the 5,5'-, 5,7'- and 7,7' isomers that are substituted at the 5-position and 7-position, were isolated and purified by column chromatography. The structures of the separated monomers were analyzed by proton nuclear magnetic resonance (^1H NMR) and Fourier transform infrared (FT-IR) spectroscopy. Electron density distribution was also calculated by the commercially available program Gaussian.

2 Experimental

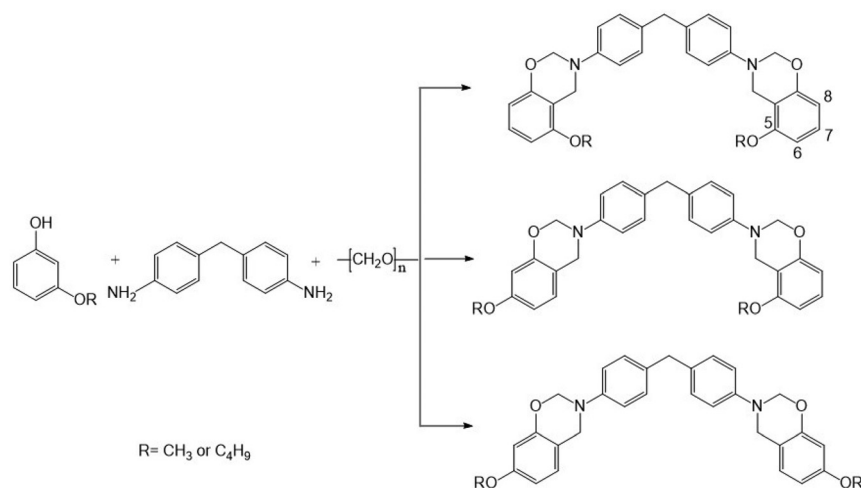
2.1 Materials

Custom synthesized *m*-butoxyphenol was received from CheMall Corp. *m*-Methoxyphenol ($\geq 95\%$) and 4,4'-diaminodiphenylmethane ($\geq 97\%$) (DDM) were purchased from Aldrich. Paraformaldehyde (reagent grade) was obtained from Sigma-Aldrich. All solvents were obtained from Fisher Chemical and used as received.

2.2 Synthesis of bis(4-((8-methoxy)-2*H*-benzo[*e*][1,3]oxazin-3(4*H*)-yl)-phenyl)methane (abbreviated as MO-ddm)

Toluene (50 mL) was added to a mixture of *m*-methoxyphenol (7.44 g, 60 mmol), paraformaldehyde (3.9 g, 130 mmol), and DDM (5.95 g, 30 mmol) in a 250 mL round-bottom flask. The mixture was magnetically stirred and heated under reflux for 6 h. The completed reaction product was washed three times with 1 N NaOH and then three times with water. The product was dried over anhydrous magnesium sulfate, and the toluene was evaporated afterward. The resulting benzoxazine monomer theoretically includes the three isomers (5,5'-, 5,7'-, and 7,7'-). Scheme 1 shows the preparation of MO-ddm and BO-ddm.

Several reports indicated that the formation of diamine-based benzoxazine is difficult because of its poor solubility and the intermediate of the triaza structure. In a previous study, the researchers solved this problem by the use of non-polar solvents with a high boiling point, particularly xylene.⁴⁰ However, this method is not successful when *m*-methoxyphenol is used. After 5 hours of the reaction of DDM, *m*-methoxyphenol, and paraformaldehyde, the temperature was increased



Scheme 1 Synthesis of benzoxazine monomers based on *m*-alkoxyphenol and DDM yielding 5,5'- (top), 5,7'- (middle), and 7,7'- (bottom) isomers.

to 135 °C, and the mixture became a gel due to the high reactivity of the monomers formed.

Considering the reactivity of *m*-alkoxyphenol, chloroform was used as the solvent at the reflux temperature. However, it was found that the reaction product was difficult to handle because the mixture became deep colored when it was base washed and the solvent was removed. By changing the solvent to toluene, this problem was overcome. After 4 hours of the reaction using toluene, there was a little insoluble triaza structure in the mixture, which was not changed anymore over time. Therefore, the results reported in the current study are based on synthesis using toluene as the solvent.

The product was separated and purified by column chromatography with a fractional elution procedure that was applied by using a series of increasingly more polar solvents – hexane/acetone in 10:1, hexane/acetone in 5:1, and then hexane/acetone in 2:1. The column packs 40 times the sample amount of silica gel, with a height-to-diameter ratio of 8:1. Three isomers were collected, and the yield of the total isomers was 92%.

5,5'MO-ddm, ^1H NMR (CDCl_3 , 600 MHz ^1H , 298 K, δ): 3.79 (s, 8H, Ar- CH_2 -Ar and O- CH_3), 4.50 (s, 4H, N- CH_2 -Ar), 5.27 (s, 4H, O- CH_2 -N), 6.42 (ddd, $J = 20.0, 8.3, 0.9$ Hz, 4H, H-6 and H-8), 7.08–6.98 (m, 10H, Ar and H7). FT-IR spectra (KBr): 1239 cm^{-1} (C–O–C asymmetric stretching), 1077 cm^{-1} (symmetric stretching of C–O–C), and 945 cm^{-1} (benzoxazine-related band).

5,7'MO-ddm, ^1H NMR (CDCl_3 , 600 MHz ^1H , 298 K, δ): 3.73 (s, 3H, O- CH_3 at the 7-position), 3.79 (s, 5H, Ar- CH_2 -Ar and O- CH_3 at the 5-position), 4.50 and 4.52 (s, 4H, N- CH_2 -Ar), 5.27 and 5.29 (s, 4H, O- CH_2 -N), 6.34 (d, $J = 2.6$ Hz, ^1H , H-8'), 6.42 (m, 3H, H-6, H-6' and H-8), 6.87 (dt, $J = 8.4$ Hz, 1H, H-5'), 7.08–6.97 (m, 9H, Ar and H7) FT-IR spectra (KBr): 1240 cm^{-1} (C–O–C asymmetric stretching), 1104 cm^{-1} (symmetric stretching of C–O–C), and 947 cm^{-1} (benzoxazine-related band).

7,7'MO-ddm, ^1H NMR (CDCl_3 , 600 MHz ^1H , 298 K, δ): 3.73 (s, 6H, O- CH_3 at the 7-position), 3.79 (s, 2H, Ar- CH_2 -Ar), 4.52

(s, 4H, N- CH_2 -Ar), 5.30 (s, 4H, O- CH_2 -N), 6.34 (d, $J = 2.6$ Hz, 2H, H-8), 6.46 (dd, $J = 8.4, 2.7$ Hz, 2H, H-6), 6.87 (dt, $J = 8.4$ Hz, 2H, H-5), 7.08–6.97 (m, 8H, Ar) FT-IR spectra (KBr): 1239 cm^{-1} (C–O–C asymmetric stretching), 1104 cm^{-1} (symmetric stretching of C–O–C), and 978 cm^{-1} (benzoxazine related band).

2.3 Synthesis of bis(4-((8-butoxy)-2H-benzo[*e*][1,3]oxazin-3(4H)-yl)-phenyl)methane (abbreviated as BO-ddm)

In a 250 mL round-bottomed flask equipped with a magnetic stirrer, *m*-butoxyphenol (9.97 g, 60 mmol), paraformaldehyde (3.9 g, 130 mmol), DDM (5.95 g, 30 mmol), and toluene (50 mL) were added and stirred at reflux for 6 h. As the reaction mixture cooled, the raw product was washed with 1 N NaOH three times and water three times. The product was dried over anhydrous magnesium sulfate, and the toluene was evaporated afterward.

BO-ddm was separated and purified by column chromatography using a hexane/acetone mixture (10:1) as the eluent, and with a column of the same size and with the same amount of silica gel as the column used for MO-ddm separation. Two compounds were separated from the product, although theoretically, three isomers are possible: the first band collected was a yellow sticky liquid, and after the yellow band eluted completely, the second product was obtained in the form of a white powder. The yield of the total isomers was 93%.

5,7'BO-ddm, ^1H NMR (CDCl_3 , 600 MHz ^1H , 298 K, δ): 0.94–1.00 (m, 6H, $-\text{CH}_3$), 1.42–1.52 (m, 4H, $-\text{CH}_2-\text{CH}_3$), 1.69–1.79 (m, 4H, O- CH_2-CH_2), 3.80 (s, 2H, Ar- CH_2 -Ar), 3.88 (t, 2H, O- CH_2 - at the 7-position), 3.95 (t, 2H, O- CH_2 - at the 5-position), 4.50 and 4.51 (s, 4H, N- CH_2 -Ar), 5.27 and 5.28 (s, 4H, O- CH_2 -N), 6.33 (d, $J = 2.5$ Hz, ^1H , H-8), 6.41–6.45 (m, 3H), 6.85 (d, $J = 8.4$ Hz, ^1H , H5), 7.07–6.97 (m, 9H, Ar and H7). FT-IR spectra (KBr): 1240 cm^{-1} (C–O–C asymmetric stretching), 1106 cm^{-1} (symmetric stretching of C–O–C), and 951 cm^{-1} (benzoxazine-related band).

7,7'BO-ddm, ^1H NMR (CDCl_3 , 600 MHz ^1H , 298 K, δ): 0.95 (t, 6H, $-\text{CH}_3$), 1.42–1.49 (m, 4H, $-\text{CH}_2-\text{CH}_3$), 1.70–1.76 (m, 4H, $\text{O}-\text{CH}_2-\text{CH}_2-$), 3.79 (s, 2H, $\text{Ar}-\text{CH}_2-\text{Ar}$), 3.88 (t, 4H, $\text{O}-\text{CH}_2-$ at the 7-position), 4.51 (s, 4H, $\text{N}-\text{CH}_2-\text{Ar}$), 5.29 (s, 4H, $\text{O}-\text{CH}_2-\text{N}$), 6.33 (d, $J = 2.5$ Hz, 2H, H-8), 6.45 (dd, $J = 2.4$ and 8.4 Hz, 2H, H-6), 6.86 (dt, $J = 8.4$ Hz, 2H, H-5), 7.06–6.97 (m, 8H, Ar). FT-IR spectra (KBr): 1256 cm^{-1} (C–O–C asymmetric stretching), 1108 cm^{-1} (symmetric stretching of C–O–C), and 972 cm^{-1} (benzoxazine-related band).

2.4 Synthesis of bis(4-(2H-benzo[*e*][1,3]oxazin-3(4H)-yl)phenyl) methane (abbreviated as PH-ddm)

In a 50 mL round-bottomed flask equipped with a magnetic stirrer, DDM (5.95 g, 30 mmol), phenol (5.64 g, 60 mmol), paraformaldehyde (3.9 g, 130 mmol) and toluene (40 mL) were added and stirred at reflux for 6 h. As the reaction mixture cooled, the raw product was washed with 1 N NaOH three times and water three times. The product was dried over anhydrous magnesium sulfate, and the toluene was evaporated afterward. The product was dissolved in methylene chloride for column chromatographic purification using hexane/acetone (10 : 1) as the eluent.

PH-ddm, ^1H NMR (CDCl_3 , 600 MHz ^1H , 298 K, δ): 3.78 (s, 2H, $\text{Ar}-\text{CH}_2-\text{Ar}$), 4.57 (s, 4H, $\text{N}-\text{CH}_2-\text{Ar}$), 5.31 (s, 4H, $\text{O}-\text{CH}_2-\text{N}$), 6.77–7.10 (m, 16H, Ar). FT-IR spectra (KBr): 1226 cm^{-1} (C–O–C asymmetric stretching), 942 cm^{-1} (benzoxazine-related band).

2.5 Measurements

^1H nuclear magnetic resonance (NMR) spectra were acquired on a Varian Oxford AS600 at a proton frequency of 600 MHz. The average number of transients for ^1H NMR measurement was 64. A relaxation time of 10 s was used for the integrated intensity determination of the ^1H NMR spectra. Fourier transform infrared (FTIR) spectra were obtained using a MB300 FTIR spectrometer, which was equipped with a deuterated triglycine sulfate (DTGS) detector and a dry air purge unit. Coadditions of 32 scans were recorded at a resolution of 4 cm^{-1} . A TA Instruments differential scanning calorimeter (DSC) Model 2920 was used with a heating rate of $10\text{ }^\circ\text{C min}^{-1}$ and a nitrogen flow rate of 60 mL min^{-1} . All samples were sealed in hermetic aluminum pans.

3 Results and discussion

Syntheses of the methoxy isomers from *m*-methoxyphenol and 4,4'-diaminodiphenylmethane (DDM) are shown in Scheme 1.

3.1 ^1H NMR analysis

The structures of the isomers were analyzed by ^1H NMR. All spectra in Fig. 1 for MO-ddm show that the protons between two aromatic rings ($\text{Ar}-\text{CH}_2-\text{Ar}$) for all isomers give the signal at 3.79 ppm as a singlet. The characteristic resonances of the oxazine rings that were assigned to the $-\text{CH}_2-\text{N}-\text{Ar}$ and $-\text{O}-\text{CH}_2-\text{N}-$ protons appeared as two singlets at 4.50–4.52 and

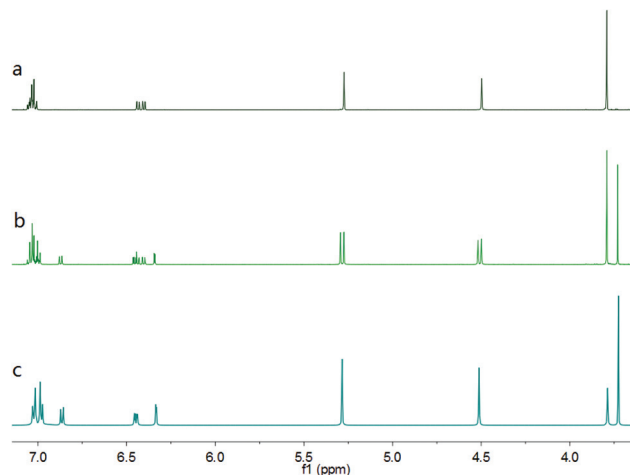


Fig. 1 ^1H NMR spectra of (a) 5,5'MO-ddm, (b) 5,7'MO-ddm, and (c) 7,7'MO-ddm.

5.27–5.29 ppm, respectively. These characteristic oxazine resonances are almost always separated by 0.8–0.9 ppm, and the observed values are in accordance with this trend.⁴ The asymmetric 5,7' isomer gave rise to two resonances in two frequency regions. This splitting was not caused by the signal splitting led by the spin–spin coupling between ^1H nuclei because there are no adjacent nuclei. The two resonances appear because of the magnetic environment inequality of these particular benzoxazine rings. The chemical shifts given by the side of the 7-position alkoxy are greater than those of the 5-position. The greater chemical shifts indicate more deshielding and less electron density of the oxazine ring. The NMR resonance has a significant influence on the ring-opening of oxazine, and therefore, is subtly related to polymerization temperature, which will be discussed in later sections.^{31,41}

The most significant difference between the three spectra of 5,5'MO-ddm, 5,7'MO-ddm, and 7,7'MO-ddm is in the range of 3.73–3.79 ppm. The integrated intensities of the 3.79 ppm resonance have different values that are in the order of 2, 1.25, and 0.5 times those of the $\text{O}-\text{CH}_2-\text{N}$ protons, which indicate that the proton numbers of these resonances are 8, 5, and 2. The integration intensities of the 3.73 ppm resonance in 5,7'MO-ddm and 7,7'MO-ddm indicate that there are 3 and 6 protons, respectively, and therefore, the resonances of 3.73 ppm are assigned to the 7-position methoxy protons. In contrast, the methoxy group at the 5-position gives rise to resonance at 3.79 ppm, which is overlapped with the signals of $\text{Ar}-\text{CH}_2-\text{Ar}$. This is why there are different values of integrated intensities at the 3.79 ppm resonance.

The different resonances of the methoxy protons in the 5- and 7-positions indicate that their environments are different because of their position on the benzene ring. The methoxy protons are influenced by the groups on the benzene rings. If the methoxy group is at the *ortho*-position of the methylamino group, the protons signal is shifted downfield and produces a resonance at 3.79 ppm; otherwise, they produce a resonance at

3.73 ppm. Finally, symmetric bis-benzoxazines-5,5'MO-ddm and 7,7'MO-ddm only have one resonance from the methoxy protons, while there are two resonances assigned to methoxy in asymmetric 5,7'MO-ddm.

The resonances of protons in the benzene ring near the alkoxy group appear at 6.34–6.45 ppm, and these are smaller than those in PH-ddm without the substituted group. Obviously, the change in resonance is caused by the alkoxy group, which affects the electron density of the benzene ring.³⁴ The study by Iguchi *et al.*³⁵ mentioned that substitution at the 7-position is favored over substitution at the 5-position in a 3 : 1 ratio. By analyzing the integration of crude MO-ddm (in the range of 6.34–7.08 ppm) into oxazine rings, we found that the concentration of the 7-position to the 5-position is a 3 : 1 ratio. According to the ratio above and column chromatography results, substitution at the 7-position is easier than that at the 5-position.

3.2 FT-IR analysis

FT-IR spectra of the *m*-alkoxyphenol-derived benzoxazine isomers obtained using the KBr pellet method are shown in Fig. 2. The existence of a benzoxazine ring aromatic ether in the monomers is indicated by the band centered at 1230–1240 cm⁻¹, which is due to the C–O–C asymmetric stretching modes. Also, the oxazine-related mode is seen in the spectrum at around 970 cm⁻¹.⁴² Furthermore, the C–O stretching vibration at round 1110 cm⁻¹ is strong in the spectrum of MO-ddm.

3.3 Polymerization behavior of *m*-methoxy functional benzoxazine monomer

The polymerization behavior of *m*-methoxyphenol-derived benzoxazine was studied by DSC, and the thermograms of the monomers are shown in Fig. 3. For each DSC curve, the endothermic thermal events between 100–150 °C were attributed to the monomer melting, while the exothermic peaks

higher than 200 °C were associated with the heat released during polymerization. Both sharp melting and polymerization peaks indicate the purity of the monomers. Two melting peaks for 5,5'MO-ddm showed crystal-to-crystal phase transition during the melting behavior.²⁵ Compared with the unsubstituted PH-ddm, the derived *m*-methoxyphenol presented lower temperatures for both the onset and maximum polymerization temperature.

In general, electron-donating groups led to a more acidic phenolic species, resulting in a stronger catalytic effect taking place and expected trend of opening the benzoxazine ring.^{43,44} *m*-Methoxyphenol is the most acidic of the three isomers and lower than phenol because the p*K*_a of *p*-methoxyphenol is higher than 10, *o*-methoxyphenol and phenol are slightly lower than 10, and *m*-methoxyphenol is around 9.6, according to the experimental and calculated p*K*_a values.^{45–47} The signals of protons in O–CH₂–N in the NMR spectrum support the above assumption. The chemical shift of protons in O–CH₂–N corresponding to the 7-position is more deshielded than the 5-position. The change in electron density in the oxazine ring seems to accelerate the ring-opening polymerization.^{35,48}

All 3 isomers have the same substituent, and the only difference between the three is the position in which the methoxy (MO) group is located. The MO group is a moderate to strong activating group that directs reactions toward the *ortho*- and *para*-positions. In compound 5,5'MO-ddm, the MO groups at both sides of the bis-benzoxazine activate two different positions, specifically the 6- and 8-positions, which are in *ortho*- and *para*-position, respectively, with respect to the position of the MO group. Thus, compared to the non-activated PH-ddm, compound 5,5'MO-ddm is more activated, and therefore, is more reactive than PH-ddm. In compound 7,7'MO-ddm, the MO groups at both sides of the bis-benzoxazine activate two different positions, specifically the 6- and 8-positions, which are both in *ortho*-position with respect to the position of the MO group. Because activation at the *ortho*-position is in

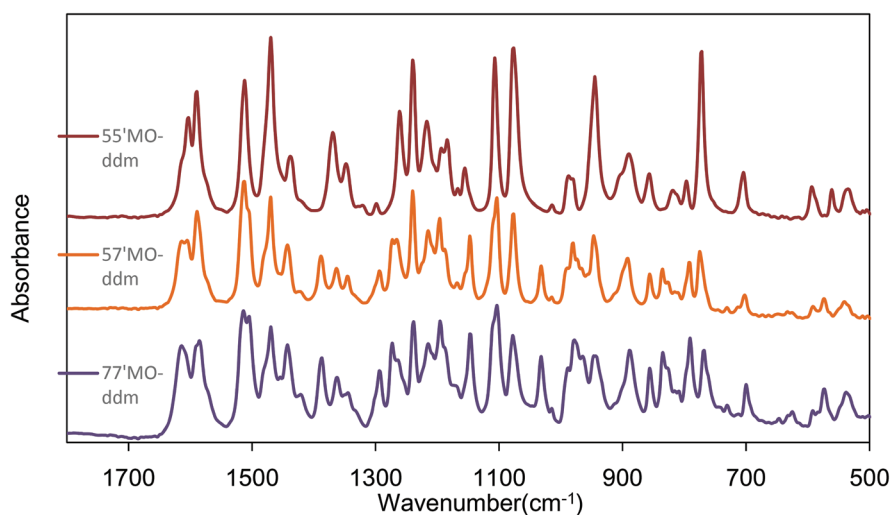


Fig. 2 FT-IR spectra of benzoxazine monomers.

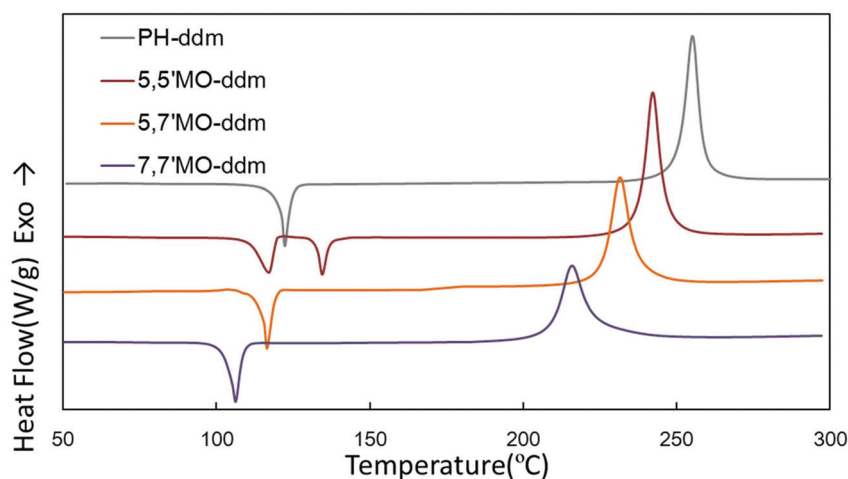


Fig. 3 DSC curves of *m*-alkoxy group benzoxazines.

general more effective than at the *para*-position for the same substituent, it can be easily understood that isomer 7,7'MO-ddm is more activated than 5,5'MO-ddm, and therefore, is also more reactive (Table 1).

It is interesting to note that the 5,7' bis-benzoxazine exhibits a polymerization exotherm close to the averaged temperature of the 5,5' and 7,7' counterparts, rather than separately showing two polymerization exotherms that correspond to pure 5,5- and 7,7-isomers. If the 5,5' and 7,7' oxazine groups are independently polymerized, the 5,7' monomer should show the onset of polymerization coinciding with 7,7' benzoxazine and the ending temperature coinciding with 5,5' benzoxazine. This is obviously not the case. Therefore, it is possible that the two benzoxazine groups are interacting in the bis-benzoxazine structure, and the electronic structure might be averaged, rather than localized. Another possibility is that the bis-benzoxazine molecule is influenced by common properties, such as molecular orientation and collision probability, which then result in an average polymerization temperature of the 5 and 7 positions, rather than two separate polymerization temperatures that correspond to those different structures. In order to obtain insights on these hypotheses, the electron density distributions of the substituted and unsubstituted bis-benzoxazines have been calculated and are shown in Fig. 4.

The electron density of the benzene ring to which the oxazine ring is attached decreases in the order of PH-ddm > 5,5'MO-ddm > 5,7'MO-ddm > 7,7'MO-ddm. In this trend, the lower the electron density on the benzene ring, the higher the

reactivity towards polymerization, and this is the opposite of what we observed for the *para*-substitution.³⁰ Hence, it is likely that for *meta*-substitution, the electron-donating group accelerates the rate of polymerization, whereas for *para*-substitution, the electron-withdrawing group will accelerate the rate of polymerization.

Table 2 lists the theoretically calculated natural charges (the sum of the electron density of the constituent carbons) of the phenolic benzene rings for all isomers of methoxy. Their values can be compared with value of the unsubstituted benzoxazine monomer, PH-ddm, which is obtained from DDM, formaldehyde, and phenol. The natural charges of the unsubstituted benzoxazine, PH-ddm, exhibit equal values of -0.76192 for the right- and left-hand side of the phenolic benzene ring. In comparison to these unsubstituted phenolic benzene rings, the methoxy-substituted phenolic-based benzoxazines exhibit significantly more positive natural charge. Such a large change in the charge density is clearly reflected in the significant temperature reduction, as well as the lowering of the activation energy of polymerization, as mentioned above. In the case of the methoxy substitution, the natural charges of the 5- and 7-position substitution are clearly shown to independently behave. The natural charges expressed in bold in the right- and left-hand sides correspond to the 5- and 7-position isomers, respectively, and they are nearly identical.

While there are some unique differences in the natural charge behavior between the methoxy-substituted phenolic structures, the clear separation of natural charge for each isomeric structure is reflected in the calculation. However, the DSC thermogram of the 5,7'-isomer displays a narrow, symmetric, and single polymerization exotherm between the 5,5'- and 7,7'-position rather than showing two peaks at the corresponding 5,5'- and 7,7' positions. At this point, two questions could be separately raised, and that is, why only one exothermic peak is observed in the DSC thermogram for the polymerization of 5,7'MO-ddm and why the polymerization temperature is between those corresponding two isomeric systems.

Table 1 The data for the DSC curves of *m*-alkoxy group benzoxazines

Sample	T_m (°C)	T_o (°C)	T_p (°C)
5,5'MO-ddm	117/134	238	242
5,7'MO-ddm	117	226	232
7,7'MO-ddm	106	209	216
PH-ddm	122	250	255

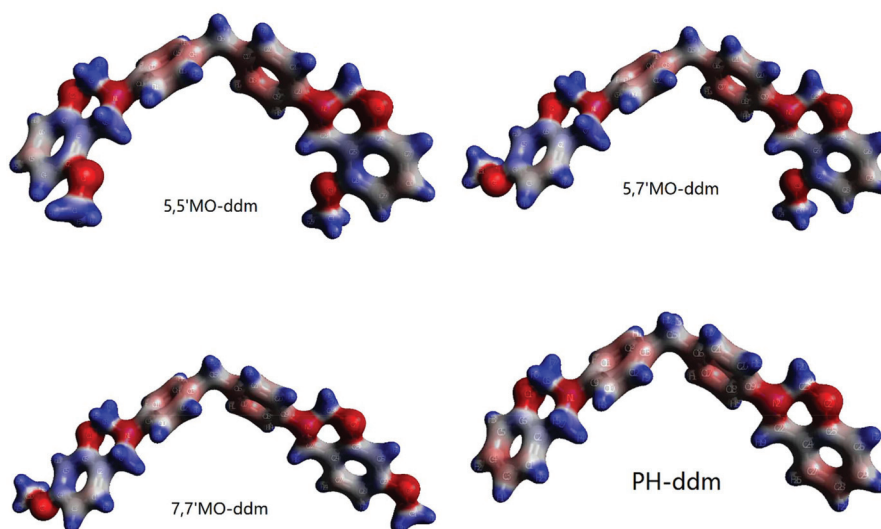


Fig. 4 The electron density distribution of the substituted bis-benzoxazines and PH-ddm.

Table 2 Electron density calculation of the methoxy-substituted phenolic benzene ring (natural charge)

Isomer	Natural charge (eV)	
	Right phenolic benzene ring	Left phenolic benzene ring
5,5'MO-ddm	−0.33404	−0.33403
5,7'MO-ddm	−0.33397	−0.33747
7,7'MO-ddm	−0.33592	−0.33735

The answer to the first question is that once the polymerization reaction is initiated, the cationic reactive species possess sufficient reactivity to react with either of the two oxazine rings belonging to the isomer 5,7'MO-ddm regardless of the magnitude of ring-opening reactivities that are individually activated by the MO groups. Thus, during the propagation step, both oxazine rings in both moieties of the asymmetric, bis-benzoxazine are indiscriminately reacting. This process might be seen as comparable to a random copolymerization, although in the current case, the two reactive oxazine rings are part of the same asymmetric 5,7'MO-ddm isomer.

To understand why one polymerization temperature was exhibited by 5,7'MO-ddm between the 5,5'- and 7,7'-positions rather than the appearance of two peaks at the corresponding 5,5'- and 7,7' positions, we need to take into consideration the rate of the reaction theory and apply it to this isomeric system. The reaction rates strongly depend on three factors: (a) the number of collisions taking place per unit time, (b) the probability of those collisions occurring at energies greater than the activation energy, and (c) the probability of collisions occurring between molecules with the appropriate spatial orientation. Clearly, any reaction condition that increases the number of collisions per unit time, such as raising the reaction temperature and increasing the concentration of reactants, increases the rate of the reaction and *vice versa*.

A closer look at the chemical structure of isomer 5,7'MO-ddm reveals that this asymmetric isomer can be seen as two independent reactive moieties linked together. The moiety bearing the MO group at the 5-position is electronically activated in the same manner as that of the less reactive isomer, which is 5,5'MO-ddm, whereas the other moiety containing the MO group at the 7'-position is electronically activated in the same manner as that of the more reactive isomer, which is 7,7'MO-ddm. However, the two moieties belonging to isomer 5,7'MO-ddm are present in the reaction medium in lower proportions as compared to those present as part of the 7,7'MO-ddm or 5,5'MO-ddm. In other words, more activated moieties can meet each other in 7,7'MO-ddm, because it is present on both sides of the molecule, whereas it is more diluted in 5,7'MO-ddm because it is present on only one side of the molecule. Being present in a lower concentration will induce a decrease in the number of collisions per unit time, making this isomer less reactive. Therefore, isomer 5,7'MO-ddm requires a higher temperature to react than the most reactive isomer, which is 7,7'MO-ddm, although not as much as required by isomer 5,5'MO-ddm.

The equimolar mixture of 5,5'MO-ddm and 7,7'MO-ddm exhibited a single polymerization exotherm at 226 °C, near the average polymerization temperature of the 5,5'- and 7,7'-position isomers. This result strongly supports the explanation proposed above.

3.4 Polymerization behavior of *m*-butoxy functional benzoxazine monomer

The NMR spectrum of BO-ddm is shown in Fig. 5. In the 5,7' BO-ddm spectrum, two groups of twin peaks at 4.50–4.52 and 5.27–5.29 ppm, which are assigned to the $-\text{CH}_2-\text{N}-\text{Ar}$ and $-\text{O}-\text{CH}_2-\text{N}-$ protons, respectively, demonstrate the asymmetric structure and influence on the difference in electron densities. The protons near the oxygen atom in the butoxy group give

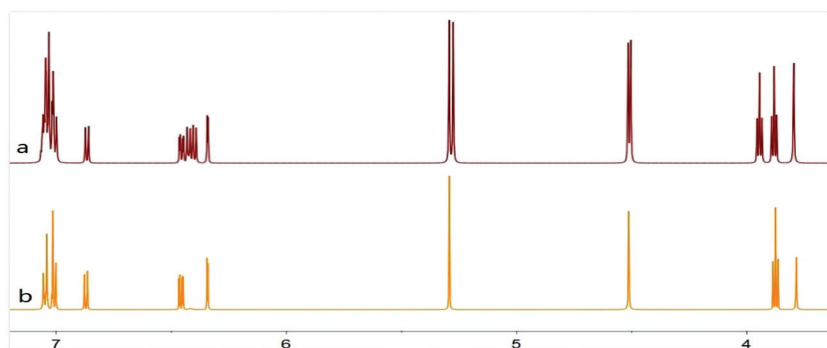


Fig. 5 ^1H NMR spectra of (a) 5,7'BO-ddm and (b) 7,7'BO-ddm.

rise to two triplets centered around 3.88 and 3.95 ppm, indicating that the environments of these protons are different. Usually, bis-benzoxazine of this size is easy to crystallize. However, the structure of 5,7'BO-ddm is asymmetric, and its side-chains are longer than those of MO-ddm, which makes it difficult to crystallize.

The NMR spectrum of crude BO-ddm (Fig. 6) shows that the integration of the 7-position butoxy is 7 times greater than that of the 5-position, which indicates that the amount of 7,7'BO-ddm is 3 times that of 5,7'BO-ddm. Furthermore, 5,5'MO-ddm was isolated through column chromatography, while 5,5'BO-ddm could not be obtained due to the very low amount in the crude product. According to the ratio above and the column chromatography results, substitution at the 5-position of the methoxy group is easier than that of the butoxy group. This is likely due to the greater steric hindrance of the butoxy group as compared to the methoxy group.

The polymerization behavior of BO-ddm benzoxazine obtained by DSC is shown in Table 3. The asymmetric 5,7'BO-ddm also has one exothermic peak similar to that of 5,7'MO-ddm, which verifies the interpretation of the polymerization mechanism of asymmetric bis-benzoxazines.

Because the extra low maxima of the polymerization temperature of 7,7'BO-ddm is impressive, the activation energies of polymerization reactions of 5,7'BO-ddm and 7,7'BO-ddm were determined by the DSC exothermic peak temperatures (T_p) as a function of the heating rate using the well-known Kissinger

Table 3 List of melting points (T_m), onset temperatures (T_o), and exotherm maxima of polymerization (T_p) obtained from the DSC thermograms of benzoxazine isomers substituted with the *m*-butoxy group

Sample	T_m ($^{\circ}\text{C}$)	T_o ($^{\circ}\text{C}$)	T_p ($^{\circ}\text{C}$)
5,7'BO-ddm	—	226	236
7,7'BO-ddm	131	196	205

and Ozawa methods.^{49,50} The plots of $\ln(\beta)$ or $\ln(\beta/T_p^2)$ against $1/T_p$ for 5,7'BO-ddm and 7,7'BO-ddm are demonstrated in Fig. 7 and 8, where b is the heating rate in $^{\circ}\text{C min}^{-1}$.

Interestingly, the E_a , shown in Table 4, is quite low at 68.0 kJ mol^{-1} (the Kissinger method) and 72.1 kJ mol^{-1} (the Ozawa method), and these are much lower than those reported for other oxygen-bearing substituted benzoxazine monomers^{51–53} and PH-ddm⁵⁴ (listed in Table 4). This activation energy of polymerization is much smaller than that of bisphenol A and aniline-based benzoxazine (abbreviated as BA-a), which is widely regarded as a standard in benzoxazine research (listed in Table 4).⁵⁵ The small activation energy of 7,7'BO-ddm indicates ease of polymerization in comparison to the activation energy for BA-a benzoxazine that has been reported in the literature. It further shows even lower values of

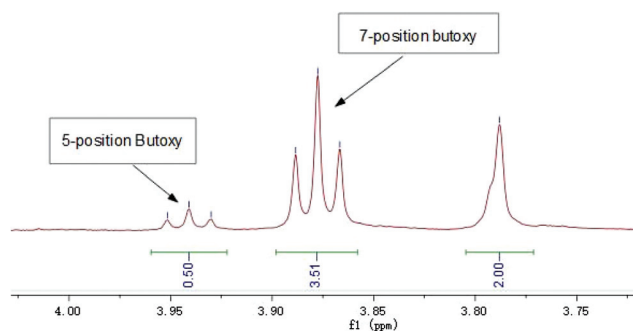


Fig. 6 ^1H NMR spectrum of crude *m*-BO-ddm.

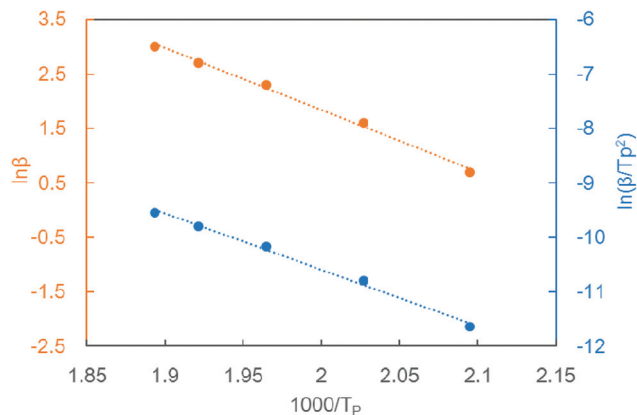


Fig. 7 Plots based on the Kissinger (●) and Ozawa (●) methods for calculating the activation energy of polymerization for 5,7'BO-ddm.

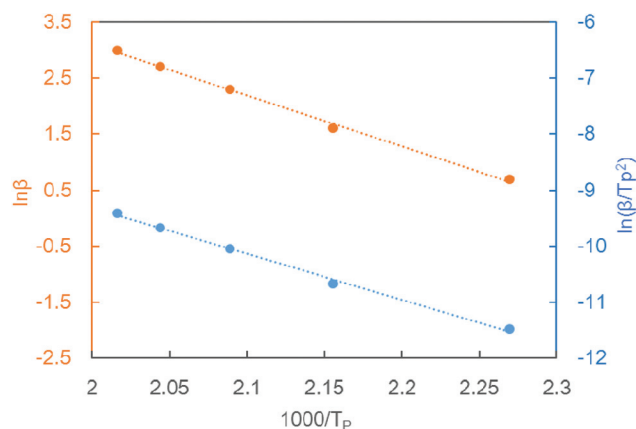


Fig. 8 Plots based on the Kissinger (●) and Ozawa (●) methods for calculating the activation energy of polymerization for 7,7'BO-ddm.

Table 4 The activation energy of 7,7'BO-ddm obtained by the Kissinger and Ozawa methods

Sample	Activation energy, E_a (kJ mol ⁻¹)		Front factor, $\ln(A)$ (s ⁻¹)
	Kissinger method	Ozawa method	
5,7'BO-ddm	86.0	89.7	5.51
7,7'BO-ddm	68.0	72.1	2.25
BA-a ^a	93.7	97.4	—
PH-ddm ^b	95.7	98.7	—

^a Data is cited from a previous study.⁵⁵ ^b Data is cited from a previous study.⁵⁴

79.8 kJ mol⁻¹ (the Kissinger method) and 81.5 kJ mol⁻¹ (the Ozawa method) for a self-catalyzed, methylol-functional benzoxazine,⁵⁶ without any obvious catalytic side groups. This situation is favorable from a shelf life point of view, because an internal catalytic group can limit the shelf life of the resin unless the catalytic group is a part of a latent catalyst structure.

4 Conclusion

The isomers of dianiline-based benzoxazines synthesized from phenols substituted in the *meta*-position by alkoxy groups were successfully separated and purified by column chromatography. Their chemical structure was confirmed by carrying out ¹H NMR and FT-IR measurements. DSC was used to further study the polymerization temperature of the series of *m*-alkoxyphenol-derived benzoxazine compounds, which showed different and much lower polymerization temperatures than the ordinary benzoxazine resins, such as BA-a. The alkoxy group acted as an electron donating substituent, which led to a more acidic phenol species and resulted in a systematic trend of benzoxazine ring-opening, and this was supported by the ¹H NMR data, which indicated deshielding of protons in the oxazine ring. A Gaussian simulation was used to determine the collective natural charge of the phenolic ring and the

oxygen in the oxazine ring of the compound. This simulation showed that the natural charge behavior exhibited some unique differences between the methoxy-substituted phenolic structures. The relationship between reaction rate and collision was applied to explain the phenomenon that asymmetric bis-benzoxazine has only one exotherm and is between the other two symmetric isomers, which was verified by polymerization of 5,7'BO-ddm. It was also found that 7,7'BO-ddm exhibits an extra low polymerization temperature and activation energy, and these were lower than those of ordinary benzoxazine monomers.

Conflicts of interest

There are no conflicts to declare.

References

- 1 C. Nair, *Prog. Polym. Sci.*, 2004, **29**, 401–498.
- 2 T. Takeichi and T. Agag, *High Perform. Polym.*, 2006, **18**, 777–797.
- 3 N. N. Ghosh, B. Kiskan and Y. Yagci, *Prog. Polym. Sci.*, 2007, **32**, 1344–1391.
- 4 H. Ishida and T. Agag, *Handbook of Benzoxazine Resins*, Elsevier, Amsterdam, 2011.
- 5 B. Kiskan, *React. Funct. Polym.*, 2018, **129**, 76–88.
- 6 M. A. Espinosa, M. Galià and V. Cádiz, *Polymer*, 2004, **45**, 6103–6109.
- 7 H.-J. Hwang, C.-Y. Lin and C.-S. Wang, *J. Appl. Polym. Sci.*, 2008, **110**, 2413–2423.
- 8 T. Zhang, H. Yan, Z. Fang and M. Peng, *Chin. J. Polym. Sci.*, 2013, **31**, 1359–1371.
- 9 C. Jubsilp, C. Panyawanitchakun and S. Rimdusit, *Polym. Compos.*, 2013, **34**, 2067–2075.
- 10 R. Sonnier, B. Otazaghine, L. Dumazert, R. Ménard, A. Viretto, L. Dumas, L. Bonnaud, P. Dubois, N. Safronava, R. Walters and R. Lyon, *Polymer*, 2017, **127**, 203–213.
- 11 J. Liu, N. Safronava, R. E. Lyon, J. Maia and H. Ishida, *Macromolecules*, 2018, **51**, 9982–9991.
- 12 S. B. Shen and H. Ishida, *Polym. Compos.*, 1996, **17**, 710–719.
- 13 H. Ishida and D. J. Allen, *J. Polym. Sci., Part B: Polym. Phys.*, 1996, **34**, 1019–1030.
- 14 H. J. Kim, Z. Brunovska and H. Ishida, *Polymer*, 1999, **40**, 1815–1822.
- 15 X. Liu and Y. Gu, *J. Appl. Polym. Sci.*, 2002, **84**, 1107–1113.
- 16 X. Liu and Y. Gu, *Acta Polym. Sin.*, 2000, **33**, 612–519.
- 17 H. Ishida and H. Y. Low, *Macromolecules*, 1997, **30**, 1099–1106.
- 18 T. Takeichi, T. Kano and T. Agag, *Polymer*, 2005, **46**, 12172–12180.
- 19 A. Chernykh, J. Liu and H. Ishida, *Polymer*, 2006, **47**, 7664–7669.

- 20 A. Trejo-Machin, P. Verge, L. Puchot and R. Quintana, *Green Chem.*, 2017, **19**, 5065–5073.
- 21 Y.-X. Wang and H. Ishida, *J. Appl. Polym. Sci.*, 2002, **86**, 2953–2966.
- 22 H. Ishida and C. M. Krus, *Macromolecules*, 1998, **31**, 2409–2418.
- 23 X. Ning and H. Ishida, *J. Polym. Sci., Part B: Polym. Phys.*, 1994, **32**, 921–927.
- 24 L. Jin, T. Agag and H. Ishida, *Eur. Polym. J.*, 2010, **46**, 354–363.
- 25 H. Ishida and P. Froimowicz, *Advanced and Emerging Polybenzoxazine Science and Technology*, 1st edn, 2017.
- 26 D. J. Allen and H. Ishida, *Polymer*, 2009, **50**, 613–626.
- 27 H. J. Kim, Z. Brunovska and H. Ishida, *J. Appl. Polym. Sci.*, 1999, **73**, 857–862.
- 28 H. J. Kim, Z. Brunovska and H. Ishida, *Polymer*, 1999, **40**, 6565–6573.
- 29 T. Agag and T. Takeichi, *Macromolecules*, 2001, **34**, 7257–7263.
- 30 X. Wang, F. Chen and Y. Gu, *J. Polym. Sci., Part A: Polym. Chem.*, 2011, **49**, 1443–1452.
- 31 S. Ohashi, D. Iguchi, T. R. Heyl, P. Froimowicz and H. Ishida, *Polym. Chem.*, 2018, **9**, 4194–4204.
- 32 L. Han, K. Zhang, H. Ishida and P. Froimowicz, *Macromol. Chem. Phys.*, 2017, **218**, 1600562.
- 33 M. Baqar, T. Agag, R. Huang, J. Maia, S. Qutubuddin and H. Ishida, *Macromolecules*, 2012, **45**, 8119–8125.
- 34 K. Zhang, P. Froimowicz, L. Han and H. Ishida, *J. Polym. Sci., Part A: Polym. Chem.*, 2016, **54**, 3635–3642.
- 35 D. Iguchi, S. Ohashi, G. J. E. Abarro, X. Yin, S. Winroth, C. Scott, M. Gleydura, L. Jin, N. Kanagasagar, C. Lo, C. R. Arza, P. Froimowicz and H. Ishida, *ACS Omega*, 2018, **3**, 11569–11581.
- 36 M. Imran, B. Kiskan and Y. Yagci, *Tetrahedron Lett.*, 2013, **54**, 4966–4969.
- 37 L. Dumas, L. Bonnaud, M. Olivier, M. Poorteman and P. Dubois, *J. Mater. Chem. A*, 2015, **3**, 6012–6018.
- 38 L. Puchot, P. Verge, T. Fouquet, C. Vancaeyzeele, F. Vidal and Y. Habibi, *Green Chem.*, 2016, **18**, 3346–3353.
- 39 R. Ganfoud, N. Guigo, L. Puchot, P. Verge and N. Sbirrazzuoli, *Eur. Polym. J.*, 2019, **119**, 120–129.
- 40 S. Gnanapragasam, S. Krishnan, H. Arumugam, M. Chavali and M. Alagar, *Adv. Polym. Technol.*, 2018, **37**, 3056–3065.
- 41 M. Arslan, B. Kiskan and Y. Yagci, *Polymers*, 2018, **10**, 239.
- 42 L. Han, D. Iguchi, P. Gil, T. R. Heyl, V. M. Sedwick, C. R. Arza, S. Ohashi, D. J. Lacks and H. Ishida, *J. Phys. Chem. A*, 2017, **121**, 6269–6282.
- 43 M. Arslan, B. Kiskan and Y. Yagci, *Macromolecules*, 2016, **49**, 767–773.
- 44 L. Han, M. L. Salum, K. Zhang, P. Froimowicz and H. Ishida, *J. Polym. Sci., Part A: Polym. Chem.*, 2017, **55**, 3434–3445.
- 45 M. F. Nielsen and K. U. Ingold, *J. Am. Chem. Soc.*, 2006, **128**, 1172–1182.
- 46 R. R. da Silva, T. C. Ramalho, J. M. Santos and J. D. Figueroa-Villar, *J. Phys. Chem. A*, 2006, **110**, 1031–1040.
- 47 K. C. Gross and P. G. Seybold, *Int. J. Quantum Chem.*, 2001, **85**, 569–579.
- 48 R. Andreu, J. A. Reina and J. C. Ronda, *J. Polym. Sci., Part A: Polym. Chem.*, 2008, **46**, 3353–3366.
- 49 H. E. Kissinger, *Anal. Chem.*, 1957, **29**, 1702–1706.
- 50 T. Ozawa, *Bull. Chem. Soc. Jpn.*, 1965, **38**, 1881–1886.
- 51 S. Ohashi, J. Kilbane, T. Heyl and H. Ishida, *Macromolecules*, 2015, **48**, 8412–8417.
- 52 M. L. Salum, D. Iguchi, C. R. Arza, L. Han, H. Ishida and P. Froimowicz, *ACS Sustainable Chem. Eng.*, 2018, **6**, 13096–13106.
- 53 K. Zhang and H. Ishida, *Polymer*, 2015, **66**, 240–248.
- 54 L. Li, Zhengzhou University, *Study On Preparation and Properties of New Benzoxazine Resins*, 2016.
- 55 I. Hamerton, L. T. McNamara, B. J. Howlin, P. A. Smith, P. Cross and S. Ward, *J. Polym. Sci., Part A: Polym. Chem.*, 2014, **52**, 2068–2081.
- 56 K. Zhang, L. Han, P. Froimowicz and H. Ishida, *React. Funct. Polym.*, 2018, **129**, 23–28.